

Design and Fabrication of a Low Cost Optical Tactile Sensor

Leila Hajshahvaladi

*Department of Electrical Engineering
Amirkabir University of Technology
Tehran, Iran*

l_hajshahvaladi@aut.ac.ir

Arsalan Amralizadeh

*Human & Robot Interaction Laboratory
University of Tehran
Tehran, Iran*

a.amralizadeh@ut.ac.ir

Amin Hamed

*Human & Robot Interaction Laboratory
University of Tehran
Tehran, Iran*

amin.hamed@ut.ac.ir

Hamed Nazemi

*Department of Mechanical Engineering
Amirkabir University of Technology
Tehran, Iran*

H.nazemi.h1376@gmail.com

Mehdi Tale Masouleh

*Human & Robot Interaction Laboratory
University of Tehran
Tehran, Iran*

m.t.masouleh@ut.ac.ir

Abstract—This paper presents the design and fabrication of an optical tactile sensor unit for the measure of the physical human-robot interaction pressure. This sensor consists of an infrared transmitter and an infrared receiver, which is covered by a soft silicone layer in the form of a pyramidal frustum. In this sensor, by applying the force to the sensor, the soft layer is deformed and the curtain within the cover closes the light way between transmitter and receiver. Then, the output voltage of the sensor varies with a proportional relation to the external force. The significant privilege of this optical tactile sensor unit can be regarded as high sensitivity, very low-cost, high reliability, easy to fabricate, very low power consumption. Hence, such a sensor unit can be used in the future for fabrication of a very low-cost smart shoe. The proposed sensor has an accuracy of 0.1N and a range of 9N.

Index Terms—Optical tactile sensor, Human-robot, Sensitivity, Silicone rubber, Smart shoe.

I. INTRODUCTION

In the last decade, humanoid robots have seen considerable developments in academic and industrial research. Industrial and humanoid robots are designed based on the physical Human-Robot Interaction (HRI) concept. These humanoid robots which was introduced as mechanical knight by Leonardo da Vinci [1], cooperate with humans in the same workspace as applications such as aided industrial manipulation, cooperative assembly, domestic work, entertainment, rehabilitation or medical applications [2]–[4] including the functional replacement for disabled people [5]–[9], walking assistance for the elderly [10] and load-carrying reinforcement for soldiers [11]. Hence, with approaching humanoid robots to human life and adapting their behavior to the behavior of humans, researchers are focusing more on tactile sensors. In this regard, the robots should possess human qualities. Accordingly, the artificial skin or tactile sensors may provide them the foregoing feature.

The skin is one of the most important and complex organs of the human body, which can detect any complex external colli-

sions. The development of advanced electronic devices which can imitate the human skins feature is a new research topic. They can possess a wide range of applications in robotics, artificial intelligence, and human-robot interfaces, that all lead to the development of electronic artificial skin [12]. In order to make artificial skin, suitable distributed tactile sensors are used to confer the sense of touch to robots [13]. Soft tactile sensors can detect the interaction behaviors occurring between the tactile robots and the humans and/or the external environment. It depends on weight and stiffness of an object as when touched, how tactile robots surface feels and deforms and how it moves when being pushed [14]. Despite their success, most humanoid projects have limitations due to the absence of satisfactory tactile sensors and their complex nature. However, production of these sensors with innovative designs is in progress [15]. In short, the following two main parts are necessitated to make a soft tactile sensor [16]:

- Firstly, the transduction mechanism is needed to detect and measure the application point of the external force

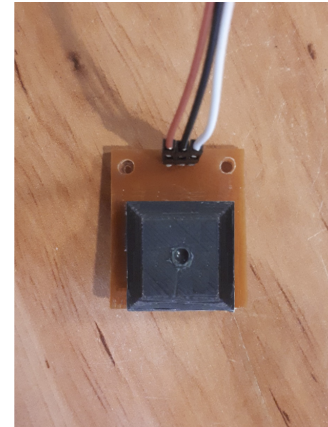


Fig. 1. The optical tactile sensor prototype.

TABLE I
THE ADVANTAGES AND DISADVANTAGES OF VARIOUS TRANSDUCTION MECHANISMS

Transduction Mechanisms	Advantages	Disadvantages
Optical	High sensitivity and reliability Wide sensing range Rapid response Low hysteresis High spatial resolution	Bulky in size Sensitive to temperature or misalignment
Capacitive	High sensitivity Large dynamic range Small in size High spatial resolution Temperature and pressure independent	Susceptible to noise High hysteresis Cross-talk between elements
Piezoresistive	Good sensitivity Simple construction Low cost High spatial resolution Low noise	Nonlinear output High hysteresis High power consumption
Piezoelectric	High sensitivity Large dynamic range High accuracy High frequency response	Sensitive to temperature Charge leakages Low spatial resolution Response to dynamic forces
Magnetic	High sensitivity Good dynamic range Linear output	Sensitive to noise Susceptible to magnetic fields

to the sensor.

- Secondly, the transduction mechanism needs to be covered by a soft and flexible deformable layer in order to transfer the external force into mechanical deformation, which enable to be measured.

Tactile sensors have been studied using various transduction mechanisms, including optical [2]–[4], capacitive [17]–[19], piezoresistive [20], [21], piezoelectric [22], [23] and magnetic [24], [25]. A summary of the advantages and disadvantages of these transduction mechanisms is provided in Table I. Among the mentioned mechanisms, optical tactile sensors have the principal benefits of the high sensitivity, good reliability, rapid response, the more comfortable assembly procedure, the feasibility of integrating a large number of sensing elements on a single device, low-cost, compatibility to mechanical structures characterized by limited stiffness, lack of hysteresis and the intrinsic robustness with respect to electromagnetic noise. Therefore, optical soft sensors are extremely convenient for design and fabrication of the artificial skin and smart shoe. Although, these sensors may be slightly bulky in size rather than other sensors [26]. Furthermore, many of these soft sensors use silicone rubber as a deformable element for the soft layer in the structure of their sensors due to unique properties such as its high rubber feature, high durability, ease of use and low cost [16].

The idea of using optical tactile sensors that can measure normal as well as shear forces was originally proposed in [27], but it has not been integrated into a robotic system yet. Then

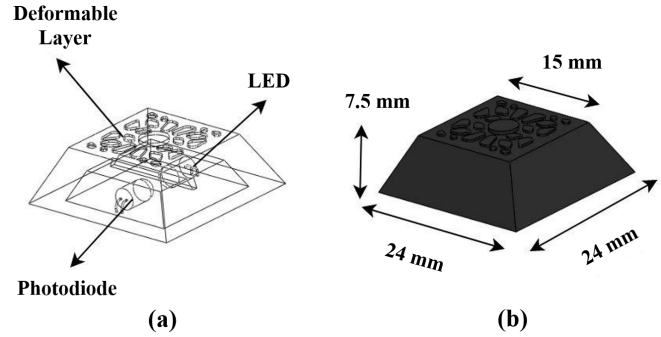


Fig. 2. (a) Schematic view and (b) occupied area of the proposed optical tactile sensor unit.

in [28], the design and realization of a conformable tactile sensor skin composed of multiple modules is proposed. The developmental process of a new tactile sensor based on the use of Light Emitting Diode (LED) and phototransistor couples that are covered by a silicone rubber layer positioned above the optoelectronic devices, was presented in [29]. Other similar works described in [2], [13], [30]–[35] have the potential to be integrated into robotic applications. Among these, the highest sensitivity and the maximum force/pressure range are about 0.036mN and 14-16N, respectively.

In this paper, the prototype of an optical tactile sensor unit for the measure of the physical human-robot interaction pressure is presented. This prototype is shown in Fig. 1, which the sensitive element consists of an infrared optical emitter/receiver couple and it is covered by a silicone layer transducing the external force in a mechanical deformation. When a force is applied onto the soft surface, the curtain within the cover closes the light way. By altering the light intensity, the output voltage of the sensor varies. This variation is proportional to the external pressure and force applied onto the soft surface. To this end, the proposed sensor is experimentally calibrated and tested. The significant privilege of this optical tactile sensor unit is in terms of its high sensitivity, very low-cost, high reliability, easy to fabricate, very low power consumption, resistance to excessive force, low hysteresis, lack of noise. Also, by varying the shape and thickness of the deformable layer, the force range and accuracy can be adjusted for different applications. Hence, such a sensor unit can be used in the future for fabricating of a very low-cost smart shoe.

The rest of this paper is organized as follows. In Section II, the working principle of the proposed optical tactile sensor, electrical description, deformable layer and Finite Element (FE) simulation are explained. In Section III, the performance of the fabricated sensor is expressed by calibrating and applying different loads to the sensor. Finally, Section IV is dedicated to the conclusion and future work.

II. WORKING PRINCIPLE

In this section, the working principle of the proposed optical tactile sensor is explained. Then, the evolution of the design of

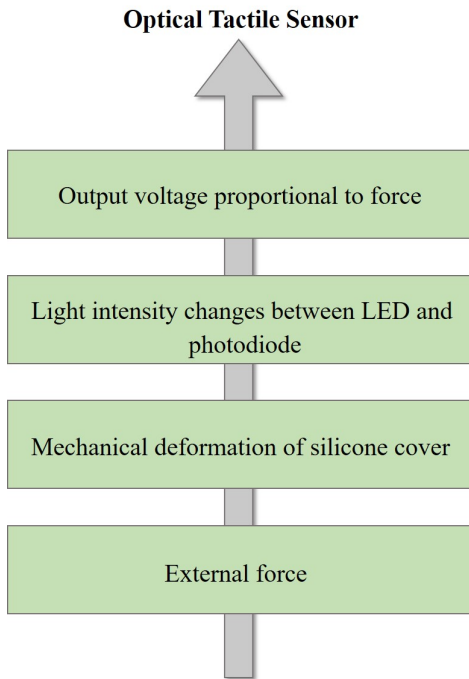


Fig. 3. The steps of the working principle of an optical tactile sensor.

the desirable sensor is expressed, along with their mechanical and electrical characterization. The proposed sensor is an optical tactile pressure sensor unit made of the following two main parts:

- a Printed Circuit Board (PCB)
- a silicone cover

The sensitive element is composed of an infrared LED in front of a Photo Diode (PD) on the same plane (mounted on the PCB). LED and PD are infrared transmitter and receiver, respectively. This sensitive element is covered with a silicone deformable layer, which is glued onto the PCB. The shape of the cover is a pyramidal frustum with a square basis, with an internal curtain in the center. The schematic view and the occupied area of the proposed optical tactile sensor unit are shown in Fig. 2.

The occupied area of the frustum base is $24 \times 24\text{mm}^2$, while the area of the top face is $15 \times 15\text{mm}^2$, and the height is 7.5mm. This sensor can be adjusted based on the limitations of specific applications. Thus, it can be employed in custom sizes.

The steps of the working principle of an optical tactile sensor are demonstrated in Fig. 3. When a force is applied onto the frustum top surface, the soft silicone layer is deformed and the curtain within the cover closes the light way between LED and PD. Then, by altering the light intensity, the photocurrent measured by the PD changes. Therefore, the output voltage of the sensor proportional to external pressure and force varies.

A. Electrical Description

Figure 4 illustrates the overview of the proposed optical tactile sensor mounted onto a custom single-layer PCB of size

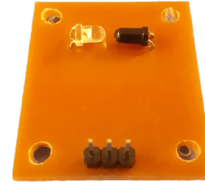


Fig. 4. The overview of the proposed optical tactile sensor on the printed circuit board

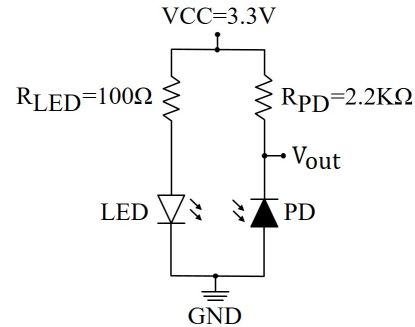


Fig. 5. The circuit schematic of the proposed optical tactile sensor.

30mm by 30mm. It is obvious that the components of the sensing element on the PCB are an infrared LED, known as the 3mm chip with a viewing angle of 40 deg, and an infrared PIN PD, known as the 3mm chip with a viewing angle of 45 deg. Both the components have maximum peak sensitivity at 850 nm wavelength. By concerning to the effects of the radiant intensity pattern of the LED and responsivity pattern of the PD on the photocurrent while they are facing each other inside silicone cover. For the sake of good response of the sensor, the components of LED and PD should have small viewing angles. Besides, as for biasing of the sensing element, two suitable resistors are selected. The resistor LED fixes the LED emitted light and the resistor PD converts the photodiode measured photocurrent into an output voltage signal. It is suitable for a directly Analog-to-Digital (A/D) conversion without any amplification and/or filtering stage. Also, this PCB has a total of 3 pin headers namely power (VCC), ground (GND) and output (OUT). The circuit schematic of the proposed optical tactile sensor unit is shown in Fig. 5.

B. Deformable Layer and Finite Element Simulation

Herein, the material used for the realization of the deformable layer is considered the silicone rubber due to its unique and suitable properties such as high plasticity feature, ease of use, and low cost. The deformable layer should have the following two main properties:

- The optical property (e.g., color);
- The mechanical property (e.g., thickness and hardness);

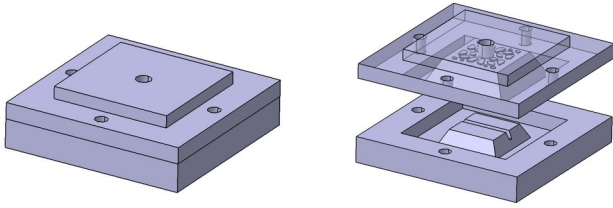


Fig. 6. The schematic of 3D printed molds.

Hence, the sensitivity of the sensor depends strongly on the optical and mechanical properties of the material used for the deformable layer.

a) *Rubber Casting*: In order to form a soft and deformable layer, RTV silicone rubber has been used with a Shore hardness of 25A. Silicone rubber is colored by black pigment silicone to guarantee a high absorption for every wavelength and to optimize the sensitivity of the sensor. For this purpose, two-piece 3D printed molds have been designed, which is depicted in Fig. 6. Before the black silicone rubber is injected into the Sprayed mold, the silicone is placed in a vacuum chamber for degassing all the trapped air. The equipment used for molding tactile sensors has referred in [16]. After the degassing step, the mold is placed in the room temperature for hours to dry silicone. The silicone cover becomes ready to be used as a deformable layer in proposed optical tactile sensor.

b) *3-dimensional finite element simulation*: Two essential parameters for making the sensor and survey its performance are as follows:

- Maximum measurable force (saturation limit)
- Sensor reversibility at high-frequency loads

The above parameters depend on factors such as the hardness of the molded silicone, the shape of the silicone cover, the frustum top surface area and designed walls of the pyramidal frustum. Figure 7 shows a cross section of the proposed silicone cover which is identified by five geometrical parameters, including thickness (T), the height of the curtain (H_1), the height of the pyramidal frustum (H_2), the side of the

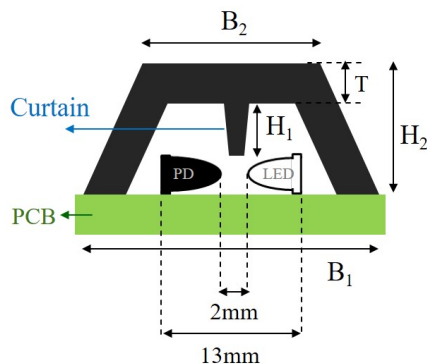


Fig. 7. Cross section of the proposed silicone cover.

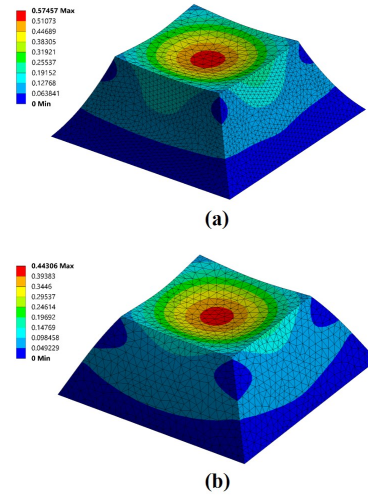


Fig. 8. The deformation of the silicone cover with (a) curved walls which the center of curvature is the outside of the sensor and (b) smooth walls by the pressure of 35kPa.

base (B_1), the side of the top-face base (B_2). The value of these parameters has to be chosen in order to obtain a soft cover with high reversibility and high saturation limit to the force applied.

Different prototypes are realized including curved and smooth walls of the frustum by utilizing the 3D-FE simulation. Both covers are simulated in the same dimension. Since the reversibility and saturation limit of cover with smooth walls are relatively higher compared to those of cover with curved walls, the cover with smooth walls is selected to be fabricated. After this prototype was fabricated, there were two significant problems:

- After loading, the sensor was slightly loose and showed no value for minimal forces.
- Sensor saturation limit was relatively low and required to be improved.

Therefore, the following practical solutions are suggested for both prototypes, including curved and smooth walls, to solve the above problems:

- In order to increase the sensor saturation limit, the center of the wall curvature was changed from the inside to the outside of the sensor, and then the thickness of the silicone cover was increased.
- The sensor did not respond to minimal forces, because the internal curtain between the LED and the force detector was short. For this purpose, the height of the curtain within the silicone cover was increased and the height of the pyramidal frustum was shortened. As a result, the end of the curtain approached the PCB surface.

According to Fig. 8(a), the deformation of the silicone cover with curved walls is investigated by the pressure of 35kPa on the surface. It can be seen from Fig. 8(a), changing the center of curvature from the inside to the outside of the sensor and growing the thickness of walls causing the

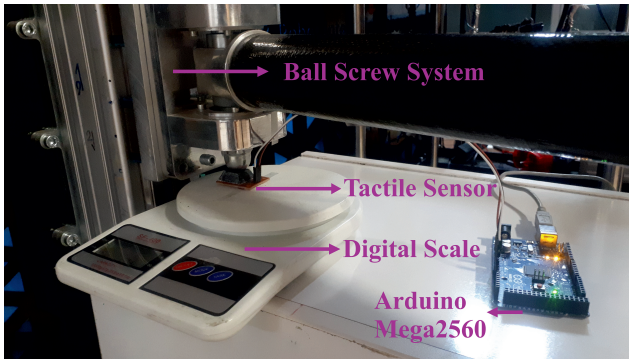


Fig. 9. Setup for calibration of proposed sensor

deformation are significantly reduced. So, the saturation limit has increased. But, by altering the height of the curtain within the silicone cover, the sensor still cannot respond well to minimal forces. Besides, the deformation of the cover with thicker smooth walls under 35kPa pressure is investigated in Fig. 8(b). In this cover, the thickness of the silicone cover has grown by about 0.7mm, the height of the curtain increased slightly, and the height of the pyramidal frustum decreased by about 0.5mm. It is observed that the response to minimal forces and the saturation limit in this cover compared to cover with curved walls improved slightly. Hence, the improved cover with smooth walls is selected. The improved geometrical parameters are listed as $T=3.5\text{mm}$, $H_1=1.5\text{mm}$, $H_2=7.5\text{mm}$, $B_1=23.7\text{mm}$, $B_2=15.7\text{mm}$. These values correspond to an average pressure of about 35kPa.

III. SENSOR CHARACTERIZATION

To assess the performance of the fabricated sensor and to find the correlation between the infrared receiver output voltage and different loads applied to the sensor, a custom setup was implemented. As shown in Fig. 9, the setup consists of a ball screw system that is used for pushing down the elastomer and a digital scale with the range of 10kg and resolution of 1g for measuring the actual amount of load exerted by the ball screw to the sensor. In this respect, the sensor is mounted on the digital scale and placed under the ball nut of the ball screw system. The ADC unit of Arduino Mega2560 is utilized for measuring the output voltage of the sensor with a sample rate of 10ms. The purpose of the loading and unloading test is to evaluate the response of the sensor for the applied force, so the experiments are performed to study the hysteresis and repeatability of the fabricated sensor.

The test started with applying a load of 30g to the surface of the cover and linearly incremented up to 900g by 30g steps and then decreased the load until the sensor unloaded entirely. The calibration result test for the proposed sensor based on different loads is shown in Fig. 10.

In Table II, the obtained results of the proposed tactile sensor was compared with the performance of other tactile sensors published in the literature. In this Table, parameters such as the accuracy, the sensing range (Range), the Output

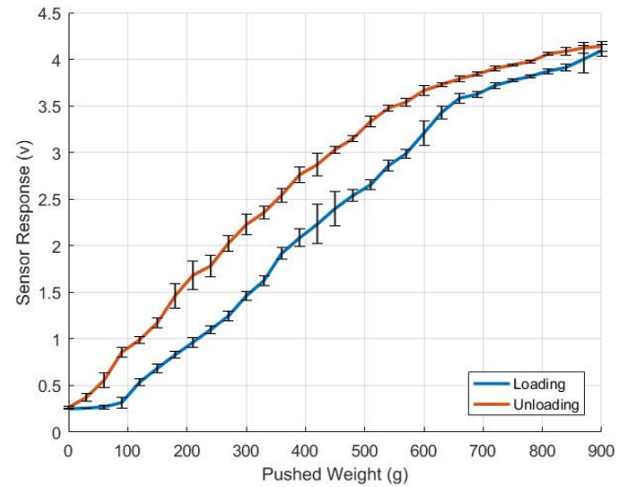


Fig. 10. The calibration test of proposed sensor based on different loads.

TABLE II
COMPARISONS BETWEEN THE PROPOSED TACTILE SENSOR AND OTHER TACTILE SENSORS.

Ref.	Accuracy	Range	Output	Cost	W	Resistance
[16]	0.01 N	4 N	I2C	6 \$	4	very low
[36]	0.3 N	300 N	Analog	3 \$	4	medium
Proposed sensor	0.1 N	9 N	Analog	1 \$	3	very high

type (Output), the cost, the number of wires (W), the resistance to excessive force (Resistance) are shown. In order to compare obtained results with those reported in Table II, the proposed tactile sensor is very low-cost, so it can be used in the future for fabricating of a very low-cost smart shoe. It also has very high resistance to excessive force, and the lowest number of wires. Beside, it has an accuracy of 0.1N and a range of 9N.

IV. CONCLUSION

In this paper, an optical tactile sensor unit for the measurement of the physical human-robot interaction pressure was introduced. Firstly, the prototype was designed and optimized by utilizing the finite element analysis, then it was fabricated. An infrared transmitter-receiver utilized, so that the sensor becomes independent of temperature. Consequently, the obtained results of the proposed tactile sensor was compared with the performance of other tactile sensors published in the literature. The proposed tactile sensor is very low-cost, so it can be used in the future for fabricating of a very low-cost smart shoe. It also has very high resistance to excessive force, and the lowest number of wires. Beside, it has an accuracy of 0.1N and a range of 9N. The proposed sensor can be easily fabricated and can be employed in custom sizes. Hence, such a sensor unit can be used in the future for fabricating a very low-cost smart shoe.

ACKNOWLEDGMENT

The authors would like to acknowledge the financial support of the Iranian National Elites Foundation, research group number 334.

REFERENCES

- [1] Gates, B., A robot in every home. *Scientific American*, 2007. 296(1): p. 58-65.
- [2] Cirillo, A., et al., An artificial skin based on optoelectronic technology. *Sensors and Actuators A: Physical*, 2014. 212: p. 110-122.
- [3] Donati, M., et al., A flexible sensor technology for the distributed measurement of interaction pressure. *Sensors*, 2013. 13(1): p. 1021-1045.
- [4] Piacenza, P., et al. Accurate contact localization and indentation depth prediction with an optics-based tactile sensor. in *2017 IEEE International Conference on Robotics and Automation (ICRA)*. 2017. IEEE.
- [5] Banala, S.K., et al. Robot assisted gait training with active leg exoskeleton (ALEX). in *2008 2nd IEEE RAS and EMBS International Conference on Biomedical Robotics and Biomechanics*. 2008. IEEE.
- [6] Schiele, A. and G. Visentin. The ESA human arm exoskeleton for space robotics telepresence. in *7th International Symposium on Artificial Intelligence, Robotics and Automation in Space*. 2003.
- [7] Walsh, C.J., K. Pasch, and H. Herr. An autonomous, underactuated exoskeleton for load-carrying augmentation. in *2006 IEEE/RSJ International Conference on Intelligent Robots and Systems*. 2006. IEEE.
- [8] Pylatiuk, C., et al. Design of a flexible fluidic actuation system for a hybrid elbow orthosis. in *2009 IEEE International Conference on Rehabilitation Robotics*. 2009. IEEE.
- [9] Kong, K. and D. Jeon. Design and control of an exoskeleton for the elderly and patients. *IEEE/ASME Transactions on mechatronics*, 2006. 11(4): p. 428-432.
- [10] Suzuki, K., et al., Intention-based walking support for paraplegia patients with Robot Suit HAL. *Advanced Robotics*, 2007. 21(12): p. 1441-1469.
- [11] Zoss, A.B., H. Kazerooni, and A. Chu, Biomechanical design of the Berkeley lower extremity exoskeleton (BLEEX). *IEEE/ASME Transactions on mechatronics*, 2006. 11(2): p. 128-138.
- [12] Wang, X., et al., Recent progress in electronic skin. *Advanced Science*, 2015. 2(10): p. 1500169.
- [13] Cavallo, A., et al., An Optoelectronic Artificial Skin for Contact Force Vector Estimation. *IFAC Proceedings Volumes*, 2014. 47(3): p. 7592-7597.
- [14] Argall, B.D. and A.G. Billard, A survey of tactile humanrobot interactions. *Robotics and autonomous systems*, 2010. 58(10): p. 1159-1176.
- [15] Dahiya, R.S., et al., Tactile Sensing-From Humans to Humanoids. *IEEE Trans. Robotics*, 2010. 26(1): p. 1-20.
- [16] Hamed, A., M.T. Masouleh, and A. Kalhor. Design and Characterization of a Bio-Inspired 3-DOF Tactile/Force Sensor for Human-Robot Interaction Purposes. in *2018 6th RSI International Conference on Robotics and Mechatronics (IcRoM)*. 2018. IEEE.
- [17] Maslyczyk, A., J.-P. Roberge, and V. Duchaine. A highly sensitive multimodal capacitive tactile sensor. in *2017 IEEE International Conference on Robotics and Automation (ICRA)*. 2017. IEEE.
- [18] Ji, Z., et al., The design and characterization of a flexible tactile sensing array for robot skin. *Sensors*, 2016. 16(12): p. 2001.
- [19] Muscolo, G.G. and G. Cannata. A novel tactile sensor for underwater applications: Limits and perspectives. in *OCEANS 2015-Genova*. 2015. IEEE.
- [20] Jung, Y., et al., Piezoresistive tactile sensor discriminating multidirectional forces. *Sensors*, 2015. 15(10): p. 25463-25473.
- [21] Duchaine, V., et al. A flexible robot skin for safe physical human robot interaction. in *2009 IEEE International Conference on Robotics and Automation*. 2009. IEEE.
- [22] Uribe, D.O., J. Schoukens, and R. Stoop, Improved tactile resonance sensor for robotic assisted surgery. *Mechanical Systems and Signal Processing*, 2018. 99: p. 600-610.
- [23] Pinna, L., A. Ibrahim, and M. Valle, Interface electronics for tactile sensors based on piezoelectric polymers. *IEEE sensors Journal*, 2017. 17(18): p. 5937-5947.
- [24] Wang, H., et al., Design methodology for magnetic field-based soft tri-axis tactile sensors. *Sensors*, 2016. 16(9): p. 1356.
- [25] Alfadhel, A., et al., A magnetoresistive tactile sensor for harsh environment applications. *Sensors*, 2016. 16(5): p. 650.
- [26] Palli, G., et al., Development of an optoelectronic 6-axis force/torque sensor for robotic applications. *Sensors and Actuators A: Physical*, 2014. 220: p. 333-346.
- [27] Yamada, K., et al. A sensor skin using wire-free tactile sensing elements based on optical connection. in *Proceedings of the 41st SICE Annual Conference. SICE 2002*. 2002. IEEE.
- [28] Ohmura, Y., Y. Kuniyoshi, and A. Nagakubo. Conformable and scalable tactile sensor skin for curved surfaces. in *Proceedings 2006 IEEE International Conference on Robotics and Automation*, 2006. ICRA 2006. 2006. IEEE.
- [29] D'Amore, A., et al., Siliconerubberbased tactile sensors for the measurement of normal and tangential components of the contact force. *Journal of Applied Polymer Science*, 2011. 122(6): p. 3757-3769.
- [30] De Rossi, S.M.M., et al. Soft artificial tactile sensors for the measurement of human-robot interaction in the rehabilitation of the lower limb. in *2010 Annual International Conference of the IEEE Engineering in Medicine and Biology*. 2010. IEEE.
- [31] Cirillo, A., P. Cirillo, and S. Pirozzi. A modular and low-cost artificial skin for robotic applications. in *2012 4th IEEE RAS and EMBS International Conference on Biomedical Robotics and Biomechanics (BioRob)*. 2012. IEEE.
- [32] Ohka, M., et al., Advanced design of columnar-conical feeler-type optical three-axis tactile sensor. *Procedia Computer Science*, 2014. 42: p. 17-24.
- [33] Ohka, M., et al. All-in-type optical three-axis tactile sensor. in *2014 IEEE International Symposium on Robotics and Manufacturing Automation (ROMA)*. 2014. IEEE.
- [34] Cirillo, A., et al., A distributed tactile sensor for intuitive human-robot interfacing. *Journal of Sensors*, 2017. 2017.
- [35] Cirillo, A., et al., Improved version of the tactile/force sensor based on optoelectronic technology. *Procedia Engineering*, 2016. 168: p. 826-829.
- [36] Shayan, A.M., et al. ShrewdShoe, a smart pressure sensitive wearable platform. in *2018 6th RSI International Conference on Robotics and Mechatronics (IcRoM)*. 2018. IEEE.